CrystEngComm

PAPER

Cite this: *CrystEngComm*, 2014, **16**, 10300

Supramolecular interactions mediated conformational modulation of flexible linker leading to the isolation of a metallo-macrocycle in a polyoxometalate matrix: Hirshfeld surfaces and 2D fingerprint plots†

Bharat Kumar Tripuramallu, Paulami Manna and Samar K. Das*

Received 19th August 2014,
Accepted 10th September 2014

DOI: 10.1039/c4ce01714e

www.rsc.org/crystengcomm

A novel polyoxometalate-based ion-pair compound, $[Cu(1,4\text{-bpimb})(H_2O)]_2[Mo_8O_{26}]\cdot 4H_2O$ (**1**), has been synthesized starting from the copper nitrate, flexible linker 1,4-bis[2-(2-pyridyl)imidazol-1-ylmethyl]benzene (1,4-bpimb) and sodium molybdate under hydrothermal conditions. The title compound was unambiguously characterized by single-crystal X-ray diffraction analysis, elemental analysis, IR spectroscopy, and thermogravimetric analysis, and bulk homogeneity has been proved by powder X-ray diffraction studies. The supramolecular interactions governed by the octamolybdate anion mediate the conformational modulation of the 1,4-bpimb linker to its thermodynamically unfavorable *cis* conformation, which coordinates to the copper ion, leading to the formation of a metallo-macrocycle. The existence of the cationic metallo-macrocycle $[Cu(1,4\text{-bpimb})(H_2O)]_2^{4+}$ in the polyoxometalate matrix as ion-pair compound **1** represents a rare example. Hirshfeld surface analyses have been studied to gain deep insight into the interactions around the metallo-macrocyclic cation. Theoretical calculations have been performed partly to establish the experimental results.

Introduction

Polyoxometalates (POMs) or metal oxide-based materials are considered to be the most promising areas of research interest in modern inorganic chemistry due to their versatile applications in the fields of catalysis, medicine, molecular electronics, separation *etc.*[1] Stable POM clusters with different sizes and topologies, such as Lindquist, octamolybdate, Keggin, Dawson, Anderson, Presslyer cluster anions *etc.*, are highly explored as counter anions or as building blocks for construction of extended architectures.[2] The stabilization of these clusters (some are of spherical shape) as counter anions with diverse cations can be achieved by coulombic and non-covalent interactions.[3] Spherical POMs, owing to the presence of negatively charged oxygen atoms on their surfaces, act as supramolecular synthons in crystal engineering.[4] Several cationic crown ethers,[5] porphyrins,[6] aza-macrocycles[7] and transition metal complexes[8] are reported with POM anions, and some of these hybrid materials have been used to isolate the toxic or radioactive metals from solutions.[9]

The non-covalent interactions, in directing the self-assembly in coordination architectures through controlling the coordination geometry,[10a] the coordination mode of the linkers,[10b] *etc.* for designing the functional materials, are of immense interest to modern inorganic chemists. In contrast to supramolecular interactions involving neutral and cationic entities, the non-covalent interactions exhibited by the anions are of particular interest due to their size, shape, geometry, high solvation energies and degree of polarization.[11] Khavasi and co-workers demonstrated the anion-directed self-assembly in coordination networks through non-covalent interactions.[12] The anions can also act as templates in the self-assembly process through non-covalent interactions, as reported by Dunbar and co-workers.[13] The anions, coordinated to the metal centers inducing a self-assembly process through non-covalent interactions, were explored by Zhou *et al.*, who demonstrated that 'the larger the size of anion, steadier the coordination complexes'.[14] Apart from classical anions, large

School of Chemistry, University of Hyderabad, Hyderabad-500046, India. E-mail: skdsc@uohyd.ernet.in, samar439@gmail.com; Fax: +91 40 2301 2460

† Electronic supplementary information (ESI) available: The supramolecular interactions around the cation and anion, TGA, PXRD, IR spectroscopy, the theoretical calculation outcomes and the complete list of bond angles and bond lengths in PDF format. CCDC 1009234 contains the supplementary crystallographic data for the title compound. For ESI and crystallographic data in CIF or other electronic format see DOI: 10.1039/c4ce01714e

spherical polyoxoanions also imprint their characteristic features in the self-assembly process.[2f,g]

The conformation of a molecule is an important parameter in deciding various functional applications in diverse disciplines. In biology, the particular conformation of the single native protein (enzyme) has the ability to catalyze the substrate conversion. The relevant conformational changes of the enzyme on catalytic activity are governed by the supramolecular interactions.[15] In the field of metal–organic frameworks/coordination polymers, in many instances, the conformation of the linker can play an important role to result in the formation of either discrete molecular boxes or extended architectures.[16] More often, the flexible linkers favor the *trans* configuration unless they are compelled by an external factor, such as a metal ion coordination sphere, coordination restrictions, the geometry of the secondary linker *etc.*[17] We have shown that the steric hindrance created by the chelated coordination mode of 2,2′-bipyridine molecules around the metal ion coordination sphere results in *cis* conformation of *p*-xylylene diphosphonic acid.[18] In a similar way, Cao *et al.* and our group demonstrated the conformation change from *trans* to *cis* by introducing rigid auxiliary secondary ligands (4,4′-bipyridine or 4-pyridyl tetrazole) in the case of the flexible linker 1,4-phenylenediaceticacid.[17] We continued our studies in this direction to explore the factors affecting the conformational modulation of flexible linkers and addressed several important points, such as the role of steric hindrance at the coordination sphere, the role of the biphenyl spacer, the influence of metal ionic radii, and the effect of the linker coordination angle in the formation of diverse metal–organic framework architectures.[19]

In this context, based on the aforementioned considerations, we turned our attention to study the non-covalent interactions exhibited by the large polyoxoanion in the self-assembly process. Our previous investigations using a hexamolybdate anion resulted in the spontaneous resolution of the Cu-aza-macrocycle through helical association with the aid of non-covalent interactions.[20] The conformational control of flexible linkers through non-covalent interactions is studied in a lighter view in the literature.[21] In the present work, we have chosen a flexible ditopic linker, 1,4-bis[2-(2-pyridyl)imidazol-1-ylmethyl]benzene(1,4-bpimb), to study its conformational probabilities under the influence of non-covalent interactions exhibited by the octamolybdate anion. In this article, we report the first paradigm of the transition metallo-macrocyle $[Cu(1,4\text{-bpimb})(H_2O)]_2$ in the octamolybdate polyoxoanion matrix $[Mo_8O_{26}]$ to form the ion-pair compound $[Cu(1,4\text{-bpimb})(H_2O)]_2[Mo_8O_{26}]\cdot 4H_2O$ (**1**) (Scheme 1). The strong non-covalent interactions exhibited by the spherical polyoxoanion octamolybdate mediate the conformational change of the flexible linker 1,4-bpimb to its thermodynamically unfavored *cis* configuration. The existence of this linker in its *cis* conformation leads to the formation of the metallo-macrocycle (Scheme 1), which has been isolated in the POM matrix. In addition, a comprehensive analysis of Hirshfeld surfaces portrays the supramolecular interactions experienced by the metallo-macrocycle in the POM matrix.

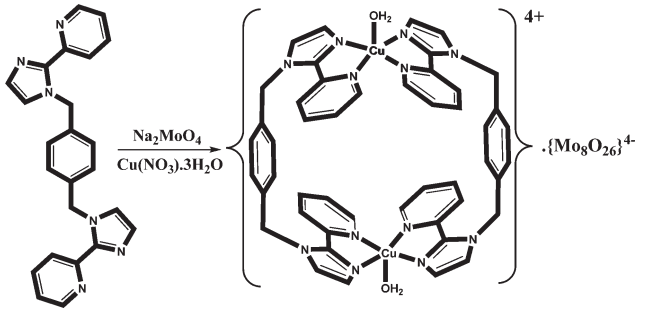

Scheme 1 Schematic representation of the linker employed and the resultant metallo-macrocycle formed in the crystal structure.

Experimental section

Materials and methods

All of the chemicals were received as reagent grade and used without any further purification. The ligand 1,4-bpimb was prepared according to the literature procedures.[22] Elemental analyses were performed by using a FLASH EA series 1112 CHNS analyzer. The infrared spectra of the solid samples were obtained with KBr pellets using a JASCO-5300 FT-IR spectrophotometer. Thermogravimetric analyses were carried out using an STA 409 PC analyzer and the corresponding masses were analyzed by using a QMS 403 C mass analyzer under the flow of N_2 gas with a heating rate of 5 °C min^{-1} in the temperature range of 30–900 °C. Powder X-ray diffraction patterns were recorded on a Bruker D8-Advance diffractometer using graphite monochromated CuKα1 radiation (1.5406 Å) and Kα2 radiation (1.54439 Å).

Synthesis of $[Cu(1,4\text{-bpimb})(H_2O)]_2[Mo_8O_{26}]\cdot 4H_2O$ (1). A mixture of sodium molybdate dihydrate (0.10 mmol, 0.242 g), copper nitrate trihydrate (0.20 mmol, 0.048 g), 1,4-bpimb (0.4 mmol, 0.157 g), and water (555.5 mmol, 10.0 g) with a mole ratio of 1 : 2 : 4 : 5555 was prepared and stirred for 30 min. Then, the pH of the reaction mixture was adjusted to 2.5 with 0.5 M HNO_3. The solution was then transferred to a 23 mL Teflon-lined autoclave in a stainless steel vessel, heated at 180 °C for 72 h and cooled to room temperature over 2 days to give blue block crystals of the title compound along with a little blue powder. Yield: 0.10 g (38%, based on copper). Anal. calc. for $C_{48}H_{52}Cu_2Mo_8N_{12}O_{32}$ (2203.62): C, 25.97; H, 2.36; N, 7.57. Found: C, 25.32; H, 2.01; N, 7.22. IR (KBr pellet) (υ/cm^{-1}): 3128, 2359, 2340, 1607, 1475, 1441, 1423, 1294, 1195, 1155, 941, 904, 855, 835, 794, 780, 727.

Single-crystal X-ray structure determination of the compounds

A single crystal suitable for structural determination of the title compound was mounted on a three-circle Bruker SMARTAPEX CCD area detector system under a Mo-Kα (λ = 0.71073 Å) graphite monochromated X-ray beam with a crystal-to-detector distance of 60 mm and a collimator of

0.5 mm. The scans were recorded with a ω scan width of 0.3°. Data reduction was performed by using SAINTPLUS;[23a] empirical absorption corrections using equivalent reflections were performed by using the program SADABS,[23b] and the structure solution was performed using SHELXS-97[23c] and the full-matrix least-squares refinement using SHELXL-97.[23d] All of the non-hydrogen atoms were refined anisotropically. Hydrogen atoms on the C atoms were introduced on calculated positions and were included in the refinement riding on their respective parent atoms. The hydrogen atoms for the solvent water molecules in the crystal structure could not be located through Fourier electron density map, although they were included in the molecular formula and molecular mass. The maximum and minimum main axis ADP ratio of the oxygen atoms O6 and O2, carbon atoms C1 and C15 and nitrogen atom N2 is more than 5.0, indicating the unresolved disorder. However, no appropriate model (by applying restraints ISOR or SIMU to displacement parameters) has been found to resolve this problem. POMs are known to show this type of unresolved disorder problems that are very common in the literature.[24] Crystal data and structure refinement parameters for the title compound are summarized in Table 1, hydrogen bonding parameters are shown in Table 2 and the complete list of bond lengths and bond angles are presented in section 4 of the ESI.†

Table 1 Crystallographic details and refinement parameters

	$[Cu(1,4\text{-bpimb})(H_2O)]_2[Mo_8O_{26}]\cdot 4H_2O$
Empirical formula	$C_{48}H_{52}Cu_2Mo_8N_{12}O_{32}$
Formula weight	2203.62
T (K)/λ (Å)	100(2)/0.71073
Crystal system	Monoclinic
Space group	$P2(1)/c$
a (Å)	13.6251(14)
b (Å)	14.7386(15)
c (Å)	16.4916(17)
α (°)	90.00
β (°)	95.699(2)
γ (°)	90.00
Volume (Å^3)	3295.4(6)
Z, ρ_{calcd} (g cm^{-3})	2, 2.198
μ (mm^{-1}), F(000)	2.198/2148
θ range for data collection	1.50 to 26.00 deg
Reflections collected/unique	14 475/6296
R_{int}	0.0596
Absorption correction	Empirical
Maximum and minimum transmission	0.8101 and 0.6676
Data/restraints/parameters	6296/0/463
Goodness of fit on F^2	1.099
R_1/wR_2 [$I > 2\sigma(I)$]	0.0665/0.1380
R_1/wR_2 (all data)	0.0915/0.1479
Largest diffraction peak/hole (e Å^{-3})	2.251 and −0.915

Table 2 Geometrical parameters of the O–H···O and C–H···O hydrogen bonds (Å, °) involved in supramolecular networks of the title compound. D = donor; A = acceptor[a]

D–H···A	d(D–H)	d(H···A)	d(D···A)	<(DHA)
O(16)–H(16A)···O(9)#3	0.76(11)	1.99(11)	2.692(9)	155.0(12)
O(15)–H(15B)···O(2)#4	0.90	2.01	2.910(9)	178.9
C(20)–H(20)···O(10)#5	0.93	2.67	3.579(11)	167.4
C(21)–H(21)···O(16)#6	0.93	2.61	3.483(11)	156.0
C(22)–H(22)···O(14)#6	0.93	2.57	3.401(12)	149.5
C(14)–H(14)···O(8)#7	0.93	2.52	3.401(10)	157.1
C(12)–H(12)···O(2)#8	0.93	2.45	3.346(10)	161.1
C(11)–H(11)···O(5)#6	0.93	2.60	3.494(10)	161.0
C(11)–H(11)···O(12)#8	0.93	2.71	3.339(10)	125.6
C(11)–H(11)···O(6)#6	0.93	2.61	3.313(10)	133.3
C(9)–H(9B)···O(1)#9	0.97	2.33	3.217(11)	151.7
C(2)–H(2)···O(7)#9	0.93	2.36	3.052(11)	131.1
C(6)–H(6)···O(10)#8	0.93	2.36	3.264(11)	164.7
C(8)–H(8)···O(8)#10	0.93	2.38	3.216(11)	149.8

[a] Symmetry transformations used to generate equivalent atoms: #3 $-x+1, -y+1, -z$; #4 $x, y-1, z$; #5 $-x+1, y-3/2, -z+1/2$; #6 $-x+2, y-1/2, -z+1/2$; #7 $x+1, -y+1/2, z+1/2$; #8 $x+1, -y+3/2, z+1/2$; #9 $x+1, y-1, z$; #10 $-x+1, y-1/2, -z+1/2$.

Results and discussion

Synthesis

The title compound $[Cu(1,4\text{-bpimb})(H_2O)]_2[Mo_8O_{26}]\cdot 4H_2O$ (**1**) was synthesized in moderate yield under hydrothermal conditions by employing copper(II) nitrate salt at relatively high temperatures in an acidic pH of 2.5. The starting precursor Cu(II) ion, during synthesis, is not reduced to its lower oxidation state in compound **1**. Thus, the flexible ligand 1,4-bpimb used in this synthesis acts only as a linker and not as a reducing agent even if it has been used in relatively higher concentration. The IR spectrum shows the characteristic features of the octamolybdate anion in the region of 1000–700 cm^{-1} due to stretching vibrations of Mo–O bonds (see section 3 of the ESI† for the IR spectrum).

Description of the crystal structure

The title compound $[Cu(1,4\text{-bpimb})(H_2O)]_2[Mo_8O_{26}]\cdot 4H_2O$ (**1**) crystallizes in the monoclinic space group $P2_1/c$ (Table 1). The molecular structure consists of a cationic di-copper complex, $[Cu^{II}(1,4\text{-bpimb})(H_2O)]_2^{4+}$, and an octamolybdate anion along with four lattice water molecules (Fig. 1). In the cationic di-copper complex, both metal atoms have distorted square pyramidal geometry. The square pyramidal coordination geometry is composed of three nitrogen atoms from two 1,4-bpimb ligands, one oxygen atom from the coordinated water molecule in the basal plane, and one nitrogen atom from 1,4-bpimb in the apical position. Both 2-(1*H*-imidazol-2-yl)pyridine moieties (which will be called **imb** hereafter) attached to the *p*-xylyl moiety of the 1,4-bpimb linker adopt a chelated coordination mode resembling the coordination mode of 2,2′-bipyridine and chelate the Cu(II) metal centre, thereby blocking four coordination sites of each Cu(II) centre by two 1,4-bpimb ligands. The residual coordination site in the Cu(II) coordination sphere is occupied by the water molecule. 1,4-bpimb usually exists in *trans* conformation,[25] but in the present study, in the $[Cu(1,4\text{-bpimb})(H_2O)]_2^{4+}$ cationic complex, it exists in a rare

cis conformation. The terminal **imb** moieties attached to the central *p*-xylyl moiety of the linker 1,4-bpimb are twisted with respect to each other by a synperiplanar torsion angle of 2.34° (viewed through N3–C23–C9–N16), and these same **imb** rings are twisted with respect to the middle *p*-xylyl moiety by a synclinal torsion angle of 63.73° and 65.53°. The synperiplanar configuration of **imb** rings imparts a *cis* conformation to the 1,4-bpimb linker, which results in the formation of a metallo-macrocycle in the cationic complex (Scheme 1 and Fig. 2). The chemistry of metallo-macrocycles is found to be very interesting because of their tendency to form different molecular polygons, *e.g.*, squares, triangles and rectangles,[26] as well as their applications in the molecular recognition and catalysis.[27] The cationic metallo-macrocycle in compound **1** has been isolated with a largely explored isopolyanion, octamolybdate. The octamolybdate anion $[Mo_8O_{26}]^{4-}$ is well characterized in the literature with α–η isomers,[2f] and in the relevant compound (present work), octamolybdate exists in its β form. As shown in Fig. 1, the β-octamolybdate is composed of eight edge-sharing MoO_6 octahedra, out of which six octahedra are characterized by two terminal oxygen atoms (O_t) attached to each Mo atom and each of the remaining two Mo octahedra has one O_t. Overall, the cluster consists of six μ_2-oxygen (O_b) atoms, four μ_3-oxygen (O_b) atoms and two μ_4-oxygen (O_b) atoms along with the terminal oxygen atoms. All of the Mo–O_t and Mo–O_b bond lengths and bond angles are in good accordance with the relevant literature values for reported β-octamolybdates (Table 1, section 4 of the ESI†).[2b] Both cationic and anionic components of the crystal structure are packed in an individual columnar arrangement; each cationic column is surrounded by four anionic columns and *vice versa* as shown in Fig. 3 (when viewed through a crystallographic *bc* plane looking down a crystallographic *a* axis). A close inspection of the packing diagram reveals an interesting pattern: the cationic columns are arranged in different configurations with respect to adjacent rows, *i.e.* all of the cationic columns

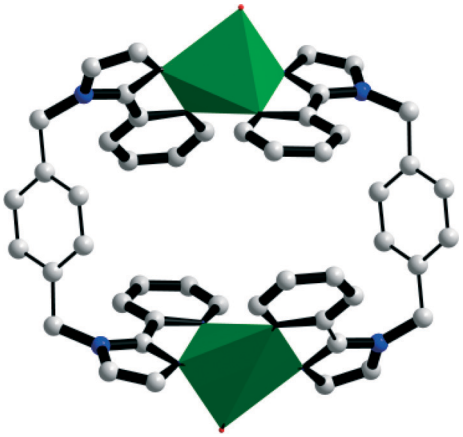

Fig. 2 Metallo-macrocycle, formed due to *cis* connectivity of the 1,4-bpimb linker, showing the polyhedral representation around the Cu(II) coordination sphere.

along the same row have an identical configuration, but these columns are tilted to another configuration in the adjacent rows. In other words, the columnar arrangements in alternative rows have the same configurations. These two different configurations are designated as 'A' and 'B' (for cations) in Fig. 3. The same pattern is also observed for the anion (octamolybdate) in the packing diagram.

The linker 1,4-bpimb, employed in the formation of cationic complex in the present study, usually exists in the thermodynamically favorable *trans* conformation (Scheme 2) as far as literature reports are concerned.[25] Thus, the occurrence of this flexible linker in the present work in a rare *cis* conformation is the key point to form the resulting metallocycle in the POM matrix. Attention should be paid to the driving force of the *cis* form of the 1,4-bpimb linker that results in the formation of the metallocycle because the *trans* form of the linker cannot logically form this metallocycle. The conformational control of the flexible linkers in the metal coordination architectures is often governed by several

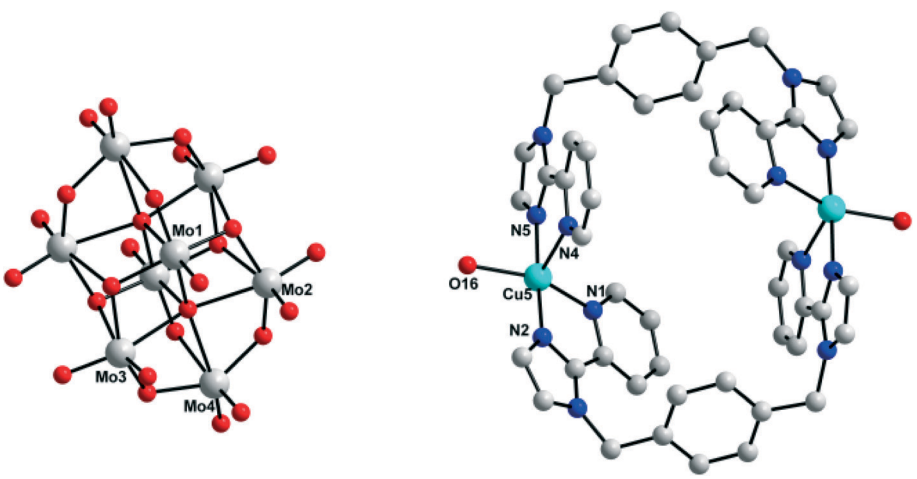

Fig. 1 Ball and stick representation of the molecular diagram of $[Cu(1,4\text{-bpimb})(H_2O)]_2[Mo_8O_{26}]\cdot 4H_2O$ (hydrogen atoms and lattice water molecules are removed for clarity).

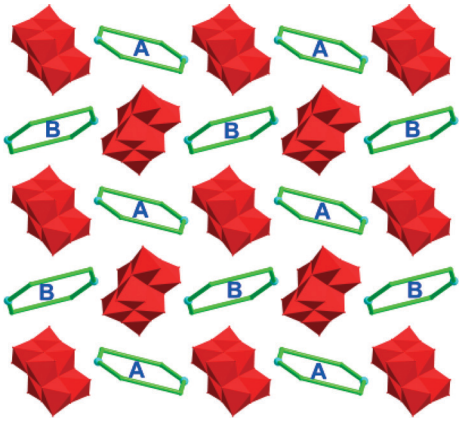

Fig. 3 Packing diagram of anionic octamolybdate and cationic metallo-macrocycle (in topological representation) components in the crystal structure viewing the different configurations of metallo-macrocycles.

important factors, for example, the coordination space available at the metal coordination sphere, the geometry of the secondary linker *etc.* However, in the present study, the absence of these factors complicates the situation that favors the formation of *cis* configuration of the linker, which is essential for metallocycle formation. We wish to address this situation by taking supramolecular interactions (see Table 2 for interaction parameters) between the cationic and anionic components in the crystal structure into account. Strong C–H···O hydrogen bonding interactions are observed between the C–H groups of the 1,4-bpimb linker and oxygen atoms of the octamolybdate anion (see Scheme 2 for the interaction sites). Among all C–H···O interactions, the key interactions exhibited by the carbon atoms C6 and C20 of the pyridine rings in the **imb** moieties with the oxygen atom O10 of the octamolybdate anion (C6–H6···O10, $d_{C\cdots O}$ = 3.264(11) Å with symmetry operator $x + 1, -y + 3/2, z + 1/2$, and C20–H20···O10, $d_{C\cdots O}$ = 3.579(11) Å with symmetry operator $-x + 1, y - 3/2, -z + 1/2$) maintain the **imb** moieties towards the same direction (Fig. 4a). In addition to these interactions, the aromatic carbon atoms (C11, C12) of the central *p*-xylyl moiety exhibit a strong interaction with the oxygen atoms (O2, O5, O6 and O12) of the same octamolybdate anion, which in turn restricts the rotation of the **imb** moieties towards the *trans* direction, which are controlled by the C(6)···O(10) and C(20)···O(10) interactions. These four interactions primarily restrict the thermodynamically stable *trans* configuration and stabilize the 1,4-bpimb linker in the *cis* configuration (Fig. 4a). Along with these interactions, the CH_2 groups of the *p*-xylyl group, the CH groups of the imidazole rings and the pyridine rings of **imb** moieties are hydrogen-bonded to both the terminal and the bridging oxygen atoms of octamolybdate anions. Overall, the *cis* configuration of each 1,4-bpimb linker in the crystal structure is stabilized by five (surrounding) octamolybdate anions through strong supramolecular interactions (Fig. 4b). There also exist strong O–H···O hydrogen bonding interactions between coordinated water molecules at the Cu(II) metal center in the metallo-macrocycle to the μ_2-oxygen atoms in the octamolybdate anion (see Fig. S1, ESI†). In total, each metallo-macrocycle is surrounded by eight octamolybdate anions through C–H···O interactions and O–H···O interactions (Fig. 5). In a similar way, each octamolybdate cluster anion is surrounded by eight metallo-macrocycles through C–H···O interactions (see Fig. S2, ESI†). The lattice water molecules are wrapped up in the dense supramolecular interactions. In a nutshell, the above-described densely packed supramolecular interactions by the octamolybdate anions stabilize the *cis* conformation of the 1,4-bpimb linker leading to the formation of the metallo-macrocycle.

When bidentate flexible linkers are employed in a framework containing compound synthesis, a wide range of coordination architectures are expected to be formed, for example, metallocycles, helicates and 2D coordination sheets; interconversion between these structures are also observed.[28] Zur Loye and co-workers reported a macrocycle and open-chain structures of a flexible benzimidazole linker demonstrating the ring-opening supramolecular isomerism based on the conformation of the ligand and the number of halogen atoms coordinating to the metal center.[16] James *et al.* also reported the ring-opening polymerization from coordination cages to coordination networks based upon the bulkiness of the linker employed.[29] These results indicate that the self-assembly processes in forming discrete metallocycles or coordination networks are often governed by several factors, such as the geometry of the linker, the size and shape of the counterions, and the most important aspect, non-covalent interactions. These interactions not only direct the self-assembly process but also stabilize the conformations of the molecules in the resulting coordination architectures. In the present work, the title compound proves to be a rare example in terms of

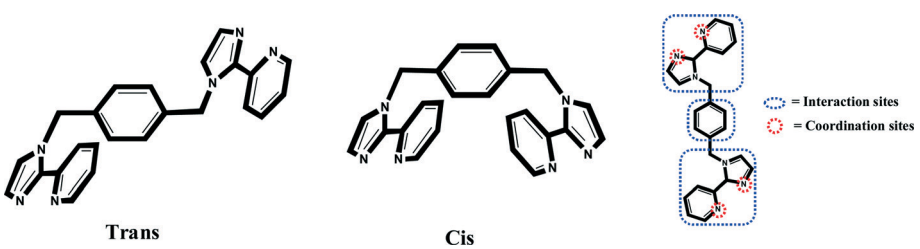

Scheme 2 *Cis* and *trans* conformations of the 1,4-bpimb linker and the blueprint representing the coordination and interaction sites.

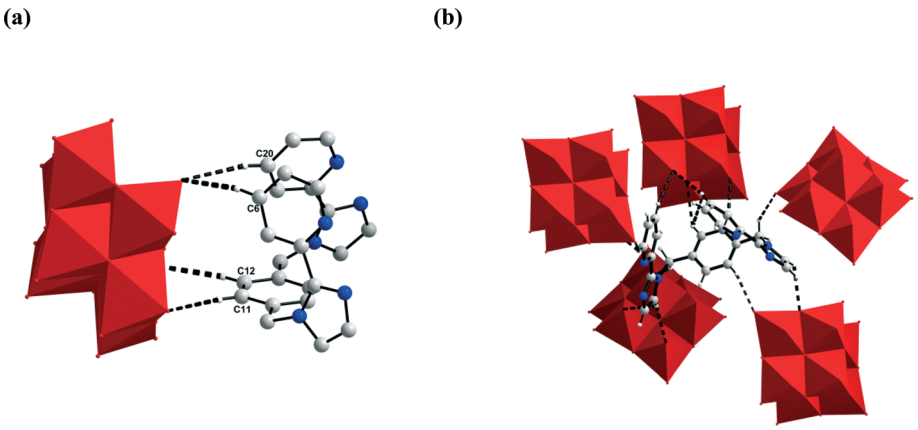

Fig. 4 (a) Key interactions that hold the 1,4-bpimb linker in *cis* configuration and (b) total interactions around the 1,4-bpimb linker.

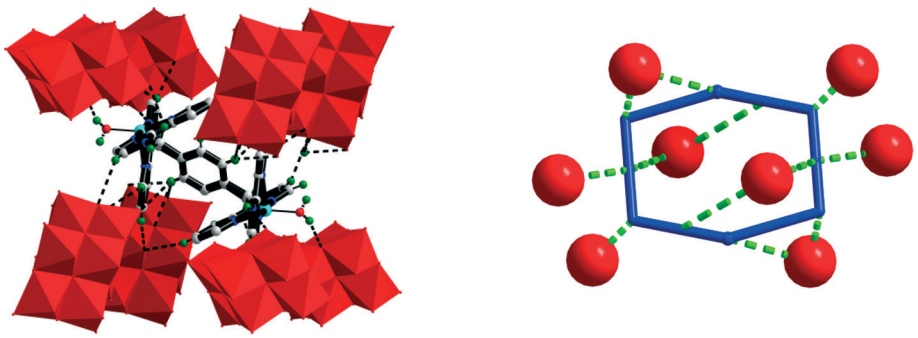

Fig. 5 Overall interactions present around the metallo-macrocyle and its understandable representation.

promoting the formation of a metallo-macrocycle through the aid of non-covalent interactions in the POM matrix.

Hirshfeld surface analysis

The dense supramolecular interactions around the metallo-macrocycle are further analyzed by studying the Hirshfeld surfaces (HSs) and 2D fingerprint plots (FPs), which are generated by using Crystal explorer 3.1 (ref. 30) based on the CIF file. The 3D Hirshfeld surfaces give additional insight into the long- and short-range interactions experienced by the molecules, and the 2D finger plot derived from the HSs gives the nature, type and relative contribution of the inter-molecular interactions. The HSs of the metallo-macrocycle in three different orientations that have been mapped over d_{norm} (−0.7 to 1.6 Å) are shown in Fig. 6a (see section 2 of the ESI† for HSs mapped with the shape index and curvedness). The surfaces are transparent to be able to visualize the metallo-macrocycle moiety. The term globularity G computed using HSs is found to be <1, indicating a structured molecular surface rather than a sphere which is similar to porphyrin structures.[31] All of the deep red spots seen in the d_{norm} surface represent the interactions, whereas the blue spots indicate the areas without close contacts. The deep red spots on each and every face of the metallo-macrocycle clearly indicate that it has been encapsulated in the dense non-covalent interactions from the octamolybdate anion. Among all of the non-covalent interactions experienced by the metallo-macrocycle, the H···O interactions (C–H···O, O–H···O) mainly dominate. These interactions are represented as sharp spikes in the 2D finger plot diagram in Fig. 6b in the 1.8 Å region (d_e + d_i). The contribution of H···O interactions (C–H···O, O–H···O) is nearly 50.3% among all interactions, which clearly gives the picture of the non-covalent interactions experienced by the metallo-macrocycle from the oxygen atoms of the octamolybdate anion. The relative contribution of different interactions are calculated and presented in Fig. 6c.

Theoretical calculations

Additionally, theoretical calculations have been performed to compare the stability of the 1,4-bpimb linker in its *cis* or *trans* conformations. The ligand geometry has been taken from the cif file and optimized; single-point energy calculations have been carried out using B3LYP with a 6–311 g** basis set (see section 2 of the ESI† for optimized structures). The optimized and the single-point energies of the 1,4-bpimb linker in *cis* conformation are −787 535.3914043 and −787 485.146025966 kcal mol^{-1}, respectively, which are higher in comparison with its corresponding energies in *trans* conformation, *i.e.* −787 542.9026943 and −787 486.826703775 kcal mol^{-1}, respectively. From the theoretical calculations, it is clearly evident that the *trans* conformation is more stable than its *cis* form and the molecule requires additional energy to stay

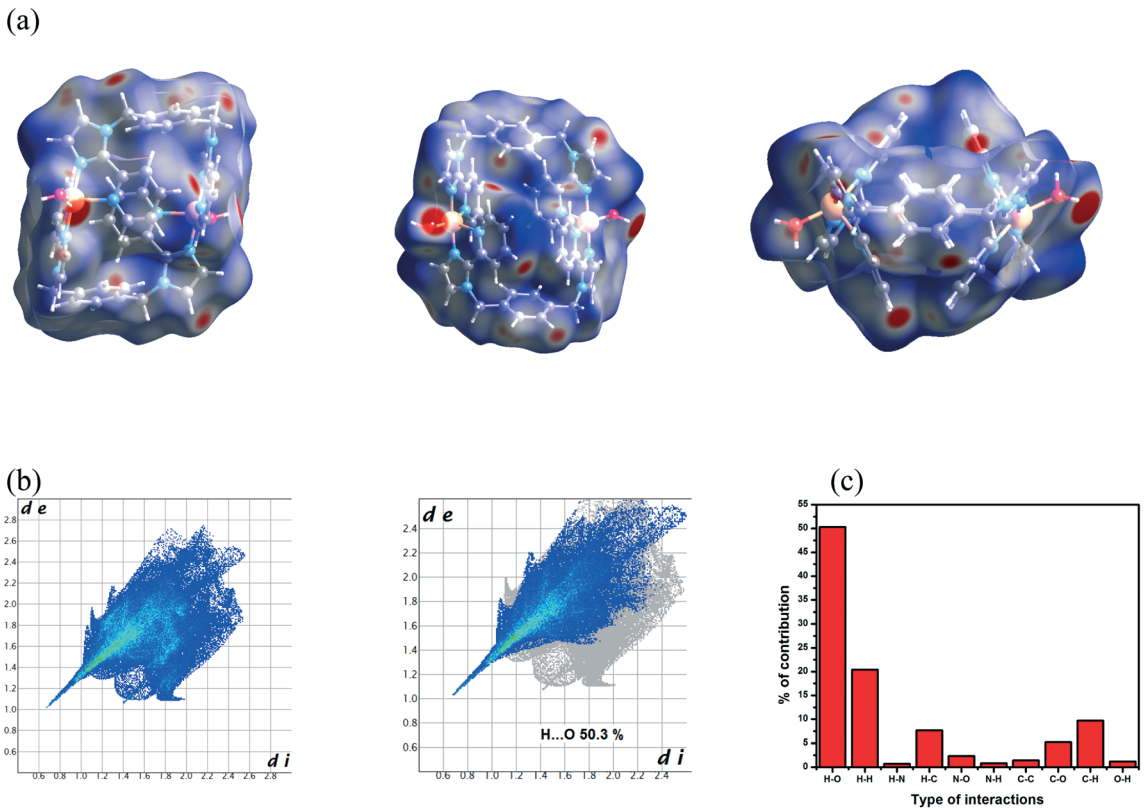

Fig. 6 (a) Hirshfeld surfaces of the title compound in three different directions, (b) 2D finger plots derived from HSs: full (left) and H···O interactions (right), and (c) percentage contribution of all interactions around the metallo-macrocyclic cation.

in the *cis* conformation. Thus, the supramolecular interactions (between the isopolyanion and the metallo-macrocycle) play an important role to stabilize the thermodynamically unfavorable *cis* conformation.

XRPD and thermogravimetric analysis

To ensure the phase purity of the title compound, the powder X-ray diffraction pattern of the powder sample has been recorded. The powder X-ray diffraction (PXRD) pattern from the simulated data is well matched with the observed PXRD pattern, proving the bulk homogeneity of the crystalline solid (see section 3 of the ESI† for PXRD patterns).

The thermal stability of the compound has been characterized by TGA studies that were performed under N_2 for the crystalline sample in the temperature range 40–1000 °C (see section 3 of the ESI† for the TGA curve). Initially, a weight loss of 2.3% was observed in the temperature regime of 40–126 °C and the compound remains stable up to 326 °C with a small weight loss of 0.6%. The total weight loss in the region of 40–126 °C is 2.9%, which can be attributed to the loss of four water molecules (theoretical weight loss, 3.2%). The dehydrated compound at 326 °C undergoes continual weight losses in two steps up to 750 °C due to coordinated water molecules in the initial stage and pyrolysis of organic ligand in the later stages with an experimental weight loss of 36.4% (theoretical weight loss, 38.1%). The residual compound at 750 °C was stable up to 1000 °C without weight loss with a weight percent of 60.45%, which is supposed to be $Cu_2Mo_8O_{26}$ (theoretical, 59.47%). The supramolecular interactions generated by octamolybdate thermally stabilize the metallo-macrocycle composite matrix to the high temperature (up to 330 °C) in comparison to conventional metallo-macrocycles.

Conclusion

In conclusion, we have reported a unique ion-pair compound, $[Cu(1,4\text{-bpimb})(H_2O)]_2[Mo_8O_{26}]\cdot 4H_2O$, with a flexible 1,4-bpimb linker. The existence of the 1,4-bpimb linker in its thermodynamically unfavorable *cis* conformation is promoted by the supramolecular interactions with the large polyoxoanion octamolybdate which leads to the formation of the metallo-macrocycle. The compound represents the first example in terms of isolation of the metallo-macrocycle in the polyoxometalate matrix. The utilization of the title compound for molecular recognition of small molecules into the cavity of the metallo-macrocycle taking the advantage of polyoxometalate is in progress.

Acknowledgements

We thank the Science & Engineering Research Board (a statutory body under the Department of Science and Technology), Government of India, for financial support (project no. SB/SI/

IC/034/2013). The National X-ray Diffractometer facility at the University of Hyderabad by the Department of Science and Technology, Government of India, is gratefully acknowledged. We are grateful to UGC, Delhi, for providing the infrastructure facility at the University of Hyderabad under the UPE grant. B.K.T and P.M. thank CSIR, India, respectively for their fellowships.

References

1 (*a*) M. T. Pope, *Heteropoly and Isopoly Oxometalates*, Springer-Verlag, Berlin, 1983; (*b*) M. T. Pope and A. Müller, *Polyoxometalate Chemistry*, Kluwer, Dordrecht, 2001; (*c*) V. Ball, F. Bernsmann, S. Werner, J.-C. Voegel, L. F. Piedra-Garza and U. Kortz, *Eur. J. Inorg. Chem.*, 2009, 5115; (*d*) Y.-Y. Bao, L.-H. Bi, L.-X. Wu, S. S. Mal and U. Kortz, *Langmuir*, 2009, **25**, 13000; (*e*) W. Bu, S. Uchida and N. Mizuno, *Angew. Chem., Int. Ed.*, 2009, **48**, 8281–8284; (*f*) C. Besson, S. Schmitz, K. M. Capella, S. Kopilevich, I. A. Weinstock and P. Kögerler, *Dalton Trans.*, 2012, **41**, 9852; (*g*) Y. Wang and I. A. Weinstock, *Chem. Soc. Rev.*, 2012, **41**, 7479.

2 (*a*) X. Kong, D. Hu, P. Wen, T. Ishii, Y. Tanaka and Q. Feng, *Dalton Trans.*, 2013, **42**, 7699; (*b*) L. Luo, H. Lin, L. Li, T. I. Smirnova and P. A. Maggard, *Inorg. Chem.*, 2014, **53**, 3464; (*c*) C.-D. Wu, C.-Z. Lu, H.-H. Zhuang and J.-S. Jin-Shun, *J. Am. Chem. Soc.*, 2002, **124**, 3836; (*d*) M.-P. Santoni, A. K. Pal, G. S. Hanan, M.-C. Tang, A. Furtos and B. Hasenknopf, *Dalton Trans.*, 2014, **43**, 6990; (*e*) R.-K. Tan, S.-X. Liu, W. Zhang, S.-J. Li and Y.-Y. Zhang, *Inorg. Chem. Commun.*, 2011, **14**, 384; (*f*) T. Arumuganathan and S. K. Das, *Inorg. Chem.*, 2009, **48**, 496; (*g*) B. K. Tripuramallu, R. Kishore and S. K. Das, *Inorg. Chim. Acta*, 2011, **368**, 132; (*h*) B. K. Tripuramallu and S. K. Das, *Cryst. Growth Des.*, 2013, **13**, 2426.

3 (*a*) V. Shivaiah and S. K. Das, *Angew. Chem., Int. Ed.*, 2006, **45**, 245; (*b*) V. Shivaiah and S. K. Das, *Inorg. Chem.*, 2005, **44**, 7313.

4 T. Chatterjee, M. Sarma and S. K. Das, *Cryst. Growth Des.*, 2010, **10**, 3149.

5 G. Bazzan, W. Smith, L. C. Francesconi and C. M. Drain, *Langmuir*, 2008, **24**, 3244.

6 (*a*) A. Yokoyama, T. Kojima, K. Ohkubo and S. Fukuzumi, *Chem. Commun.*, 2007, 3997; (*b*) A. Tsuda, E. Hirahara, Y.-S. Kim, H. Tanaka, T. Kawai and T. Aida, *Angew. Chem., Int. Ed.*, 2004, **43**, 6327.

7 (*a*) Y. Li, N. Hao, E. Wang, M. Yuan, C. Hu, N. Hu and H. Jia, *Inorg. Chem.*, 2003, **42**, 2729; (*b*) C. Streb, T. McGlone, O. Brücher, D.-L. Long and L. Cronin, *Chem. – Eur. J.*, 2008, **14**, 8861.

8 T. Akutagawa, D. Endo, F. Kudo, S.-I. Noro, S. Takeda, L. Cronin and T. Nakamura, *Cryst. Growth Des.*, 2008, **8**, 812.

9 (*a*) P. Rajec, V. Švec, V. Mikulaj and R. Hanzel, *J. Radioanal. Nucl. Chem.*, 1998, **229**, 9; (*b*) L. A. Fernando, M. L. Miles and L. H. Bowen, *Anal. Chem.*, 1980, **52**, 1115.

10 (*a*) M. Kato, K. Kojima, T. Okamura, H. Yamamoto, T. Yamamura and N. Ueyama, *Inorg. Chem.*, 2005, **44**, 4037; (*b*) D. Ghoshal, A. K. Ghosh, J. Ribas, G. Mostafa and N. Ray Chaudhuri, *CrystEngComm*, 2005, **7**, 616.

11 (*a*) R. Vilar, *Angew. Chem., Int. Ed.*, 2003, **42**, 1460; (*b*) P. D. Beer and P. A. Gale, *Angew. Chem., Int. Ed.*, 2001, **40**, 486.

12 B. Notash, N. Safari and H. R. Khavasi, *Inorg. Chem.*, 2010, **49**, 11415.

13 C. S. Campos-Fernández, B. L. Schottel, H. T. Chifotides, J. K. Bera, J. Bacsa, J. M. Koomen, D. H. Russell and K. R. Dunbar, *J. Am. Chem. Soc.*, 2005, **127**, 12909.

14 H.-P. Zhou, X.-P. Gan, X.-L. Li, Z.-D. Liu, W.-Q. Geng, F.-X. Zhou, W.-Z. Ke, P. Wang, L. Kong, F.-Y. Hao, J.-Y. Wu and Y.-P. Tian, *Cryst. Growth Des.*, 2010, **10**, 1767.

15 C. F. Rigos, H. D. L. Santos, G. Thedei, R. J. Ward and P. Ciancaglini, *Biochem. Mol. Biol. Educ.*, 2003, **31**, 329.

16 C. Y. Su, A. M. Goforth, M. D. Smith and H. C. Zur Loye, *Inorg. Chem.*, 2003, **42**, 5685.

17 (*a*) B. K. Tripuramallu, P. Manna, S. N. Reddy and S. K. Das, *Cryst. Growth Des.*, 2012, **12**, 777; (*b*) T. Liu, J. Lu, L. Shi, Z. Guo and R. Cao, *CrystEngComm*, 2009, **11**, 583.

18 B. K. Tripuramallu, R. Kishore and S. K. Das, *Polyhedron*, 2010, **129**, 2985.

19 (*a*) P. Manna, B. K. Tripuramallu and S. K. Das, *Cryst. Growth Des.*, 2012, **12**, 4607; (*b*) B. K. Tripuramallu and S. K. Das, *J. Solid State Chem.*, 2013, **197**, 499; (*c*) P. Manna, B. K. Tripuramallu and S. K. Das, *Cryst. Growth Des.*, 2014, **14**, 278; (*d*) B. K. Tripuramallu, P. Manna and S. K. Das, *CrystEngComm*, 2014, **16**, 4816.

20 (*a*) M. Sarma, T. Chatterjee, H. Vindhya and S. K. Das, *Dalton Trans.*, 2012, **41**, 1862; (*b*) M. Sarma, T. Chatterjee and S. K. Das, *Dalton Trans.*, 2011, **40**, 2954; (*c*) M. Sarma, T. Chatterjee and S. K. Das, *Inorg. Chem. Commun.*, 2010, **13**, 1114.

21 B. K. Tripuramallu, *J. Mol. Struct.*, 2014, **1071**, 79.

22 S.-L. Li, Y.-Q. Lan, J.-F. Ma, Y.-M. Fu, J. Yang, G.-J. Ping, J. Liu and Z.-M. Su, *Cryst. Growth Des.*, 2008, **8**, 1610.

23 (*a*) *SAINT: Software for the CCD Detector System*, Bruker Analytical X-ray Systems, Inc., Madison, WI, 1998; (*b*) *SADABS: Program for Absorption Correction*, G. M. Sheldrick, University of Gottingen, Gottingen, Germany, 1997; (*c*) *SHELXS-97: Program for Structure Solution*, G. M. Sheldrick, University of Gottingen, Gottingen, Germany, 1997; (*d*) *SHELXL-97: Program for Crystal Structure Analysis*, G. M. Sheldrick, University of Gottingen, Gottingen, Germany, 1997.

24 Y. Wang, L. Ye, T.-G. Wang, X.-B. Cui, S.-Y. Shi, G.-W. Wang and J.-Q. Xu, *Dalton Trans.*, 2010, **39**, 1916.

25 (*a*) Y.-Q. Lan, S.-L. Li, Y.-M. Fu, Y.-H. Xu, L. Li, Z.-M. Su and Q. Fu, *Dalton Trans.*, 2008, 6796; (*b*) G.-X. Liu, Y.-Y. Xu, Y. Wanga, S. Nishihara and X.-M. Ren, *Inorg. Chim. Acta*, 2010, **363**, 3932; (*c*) Y.-Q. Lan, S.-L. Li, J.-S. Qin, D.-Y. Du, X.-L. Wang, Z.-M. Su and Q. Fu, *Inorg. Chem.*, 2008, **47**, 10600.

26 M. Fujita, *Chem. Soc. Rev.*, 1998, **27**, 417.

27 R. V. Stone, K. D. Benkstein, S. Bélanger, J. T. Hupp, I. A. Guzei and A. L. Rheingold, *Coord. Chem. Rev.*, 1998, **171**, 221.

28 (*a*) C. Y. Su, X. P. Yang, S. Liao, T. C. W. Mak and B. S. Kang, *Inorg. Chem. Commun.*, 1999, **2**, 383; (*b*) Y. P. Cai, C. Y. Su,

C. L. Chen, Y. M. Li, B. S. Kang, A. S. C. Chan and W. Kaim, *Inorg. Chem.*, 2003, **42**, 163.
29 E. Lozano, M. Nieuwenhuyzen and S. L. James, *Chem. – Eur. J.*, 2001, **7**, 2644.
30 S. K. Wolff, D. J. Grimwood, J. J. McKinnon, M. J. Turner, D. Jayatilaka and M. A. Spackman, *Crystal Explorer 3.1 (2013)*, University of Western Australia, Crawley, Western, Australia, 2005–2013, http://hirshfeldsurface.net/CrystalExplorer.
31 (*a*) R. Soman, S. Sujatha and C. Arunkumar, *J. Fluorine Chem.*, 2014, **163**, 16; (*b*) H. M. Titi, R. Patra and I. Goldberg, *Chem. – Eur. J.*, 2013, **19**, 14941.

